Weierstraß-Institut

für Angewandte Analysis und Stochastik

im Forschungsverbund Berlin e. V.

Preprint ISSN 0946 – 8633

Relative stability of multipeak localized patterns

Andrei G. Vladimirov[1], René Lefever[2], Mustapha Tlidi[2]

submitted: 28 May 2010

[1] Weierstrass Institute
for Applied Analysis and Stochastics
Mohrenstr. 39
10117 Berlin
Germany
E-Mail: vladimir@wias-berlin.de

[2] Faculté des Sciences
Université Libre de Bruxelles
CP 231, Campus Plaine
B-1050 Bruxelles
Belgium
E-Mail: rlefever@ulb.ac.be
mtlidi@ulb.ac.be

No. 1514
Berlin 2010

2010 *Mathematics Subject Classification.* 35B36, 37L15.

Key words and phrases. Localized structures, Lyapunov functional, stability.

1999 *Physics and Astronomy Classification Scheme.* 45.70.Qj, 05.45.-a, 42.65.Pc.

Edited by
Weierstraß-Institut für Angewandte Analysis und Stochastik (WIAS)
Mohrenstraße 39
10117 Berlin
Germany

Fax: +49 30 2044975
E-Mail: preprint@wias-berlin.de
World Wide Web: http://www.wias-berlin.de/

Abstract

We study relative stability properties of different clusters of closely packed one- and two-dimensional localized peaks of the Swift-Hohenberg equation. We demonstrate the existence of a “spatial Maxwell” point where clusters are almost equally stable, irrespective of the number of pes involved. Above (below) the Maxwell point, clusters become more (less) stable with the increase of the number of peaks.

Localized patterns (LP) are nonlinear bright or dark peaks in spatially extended systems. Such patterns observed in the transverse section of coherently driven optical cavities are often called cavity solitons [1]-[6]. They are currently attracting growing interest in optics due to potential applications for all-optical control of light and for optical storage and processing of information [1]-[6]. Stationary localized peaks are independent and randomly distributed in space when they are sufficiently well separated from each other. However, when the distance between peaks decreases they start to interact via their oscillating exponentially decaying tails. This interaction then can lead to the formation of clusters [7]-[14].

In this Letter, we investigate how the number of peaks of clusters affects their stability realtively to each other. This quastion has not been addressed so far. In 1D we show numerically that there exist a “spatial Maxwell” point where all clusters are equally stable, independently of the number of constitutive peaks. Above that point, clusters become more stable as the number of peaks increases. However, beyond the “spatial Maxwell point”, clusters formed by larger number of peaks become less stable than those formed by smaller number of peaks. In 2D, we analyse the stability of hexagonal closed packed clusters with respect the number of constitutive peaks. In this case, the “spatial Maxwell” point is not a single point but rather a set of points. Apart from that, the relative stability analysis with respect to the number of peaks leads to the same conclusion as in 1D.

Our treatement is based on the Swift-Hohenberg equation (SHE) which is well known paradigmatic model. The Swift-Hohenberg equation constitutes a paradigmatic model in the study of spatial periodic or localized patterns. It has been used for that purpose in hydrodynamics [30, 24], and in other fields of natural science, such as chemistry [31], plant ecology [32], and nonlinear optics [33]. The SHE is valid close to the critical point associated with bistability and close to the symmetry breaking instability (often called Turing or modulational instability, [22]). The SHE reads

$$\partial_t U = Y + CU - U^3 - \Gamma\left(\nabla^2 U + \nabla^4 U\right), \tag{1}$$

where the Laplace operator $\nabla^2 = \partial_{xx} + \partial_{yy}$ acts in the (x,y)-plane. This equation governs the space-time evolution of the real order parameter $U(x,y,t)$ which is proportional to the deviation of the field variable from its value at the bistability threshold [23]. Y is the control parameter and C is the cooperativity.

The homogeneous steady states of Eq. (1) which satisfy the relation $Y = U_s(U_s^2 - C)$ are monostable for $C < 0$ and bistable for $C > 0$. These states undergo a symmetry breaking instability at $Y_\pm = \pm(\Gamma - 8C)U_\pm/12$, where $U_\pm = \pm\sqrt{(\Gamma + 4C)/12}$ is the amplitude U_s evaluated at the symmetry breaking thresholds. The wavelength of the pattern emerging from these bifurcation points is $\lambda_\pm = 2\sqrt{2}\pi$. Weakly nonlinear analysis of the homogeneous steady states allows us to determine the condition under which the symmetry breaking instability appears subcritically [34]. This condition is defined by the inequality $C > C_{sub} = -552\Gamma/19$. The threshold associated with the formation of localized patterns is $C = C_{sub}$. Although a weakly nonlinear analysis provides the threshold associated with appearance of localized patterns, it does not take into account the non-adiabatic effects that involve fast spatial scales responsible for their stabilization [24].

Demonstration of the existence of an infinite set of homoclinic solutions in a Hamiltonian system which is obtained by neglecting the time dependence in the SHE was the first step towards understanding of the origin of localized patterns [25]. Such homoclinic solutions correspond to stationary localized patterns with different number of peaks. More recently, the approach based on dynamical systems theory was further developed by different authors [26].

First we examine the case of one-dimensional monostable system in the subcritical regime, i.e., $C > -552\Gamma/19$. In this regime, the homogeneous steady state coexists with spacially periodic structure. In addition, the system exhibits a high degree of multistability in a finite range of parameters often called the pinning region. There is an infinite number of localized patterns each of them characterized either by an odd number $2p-1$ or even number $2p$ of peaks, where p is a positive integer. The configuration that maximizes the number of peaks in the pattern corresponds to an infinite spatial periodic distribution of the field. An example of localized patterns with $p \leq 6$ having odd and even number of peaks are shown in Figs. 1b and 1c, respectively. All patterns shown in these figures are obtained for the same parameter values and differ only by the initial condition. In the pinning region, the wavelength of the localized patterns is close to that of the periodic structure, i.e., $\lambda \approx \lambda_\pm$. Since the amplitudes of localized patterns having different number of peaks are close to one another, it is convenient to plot the L_2 -norm defined by the relation $\mathcal{N} = \int dxdy|U - U_s|^2$. Typical bifurcation diagram illustrating the dependence of $\mathcal{N}$ on the control parameter Y is shown in Fig. 1a. It consists of two snaking curves: one corresponding to LP with odd number of peaks and the other to even number of peaks in LP. As $\mathcal{N}$ increases, at each turning point where the slope becomes infinite, a pair of additional peaks appear in the pattern. It is seen from Fig. 1a that this growth is associated with back and forth oscillations around the pinning region. This behavior is referred to as homoclinic snaking phenomenon [27, 28]. More recently, homoclinic snaking behavior was observed ex-

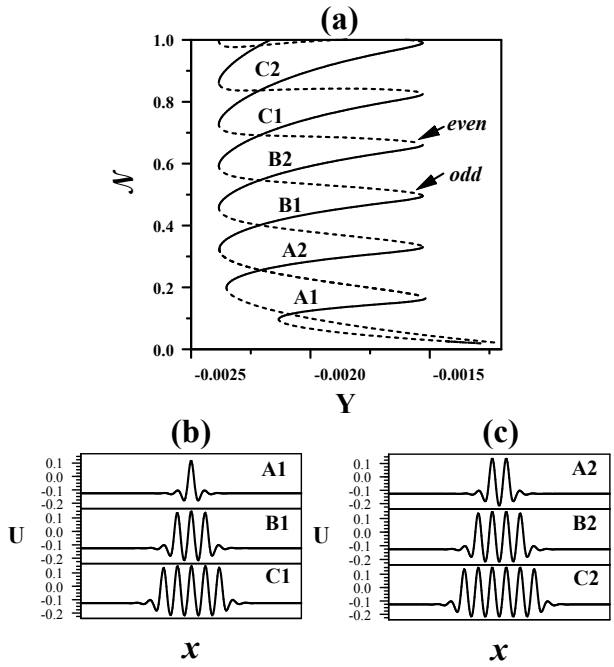

Figure 1: (a) Bifurcation diagram of Eq. (1) showing two interweaved snaking curves, one of them corresponding to odd numbers of peaks, and the other to even numbers of peaks in the localized pattern. Solid (dotted) curves correspond to stable (unstable) localized solutions. Parameters are $C = -10^{-4}$ and $\Gamma = 0.06$. (b) localized patterns with 1, 3 and 5 peaks (c) localized patterns with 2, 4, and 6 peaks. (b) and (c) are obtained for the same values of paramters and $Y = -0.002$.

perimentally [19, 20]. Relative stability analysis of the localized patterns with different number of peaks can be performed by calculating the Lyapunov functional of the SHE model defined by Eq. (1). This equation can be rewritten in the gradient form:

$$\partial_t u = -\frac{\delta \mathscr{L}}{\delta u}, \tag{2}$$

where the potential or Lyapunov functional is given by

$$\begin{aligned} \mathscr{L} &= \int dxdy \left\{ f(u) - \frac{\Gamma}{2}\left(\nabla^2 u + u\right)^2 \right\}, \\ f(u) &= -\left(C - 3U_s^2 + \frac{\Gamma}{2}\right)\frac{u^2}{2} + U_s u^3 + \frac{u^4}{4}. \end{aligned} \tag{3}$$

Since $\partial_t \mathscr{L} = -\int dxdy\,(\partial_t u)^2 \leq 0$, any initial distribution $u(x,y)$ evolves with time towards a homogeneous or an inhomogeneous (periodic or localized in space) stationary state corresponding to a local or global minimum of $\mathscr{L}$ compatible with the boundary conditions. The results of numerical calculations of the Lyapunov functional as a function of the control parameter Y are summarized in Fig. 2. Each stable localized pattern corresponds to a local minimum of the Lyapunov function. As it is seen from

the figure, there exist a “spatial Maxwell” point M located at $Y = Y_M$, where the values of $\mathscr{L}$ corresponding to different branches of stable LP coincide with a good numerical precision. For $Y < Y_M$, the Lyanunov functional $\mathscr{L}$ decreases with the decrease of the number of peaks in LP and achieves its minimum at the single peak localized solution (see branch $A1$ in Fig. 2). Therefore, localized patterns with greater number of peaks are less stable than those with smaller number of peaks in this case. At the point $Y = Y_M$ all localized patterns are equally stable, independently of the number of peaks. For $Y > Y_M$, the Lyapunov functional increases with the decrease of the number of peaks in the localized pattern. Hence, in this regime the pattern becomes more stable with the increase of the number of peaks.

In two spatial dimensions the variety of different localized patterns is much larger than in 1D. We focus on the situation where 2D peaks are hexagonal close-packed and, therefore, exert rather strong mutual forces due to their overlapping oscillatory tails. Transverse profiles of six simplest clusters are presented in Fig. 3a together with the profile of a single peak solution. These profiles have been calculated numerically by using periodic boundary conditions with different initial conditions leading to different clusters. In order to study the relative stability of clusters shown in Fig. 3a, we have calculated the dependencies of the Lyanunov functional $\mathscr{L}$ on the control parameter Y for each of these clusters. The results of are shown in Fig. 3b. From this figure we see that the four lines corresponding to the clusters B, C, D, and F intersect in a single point M2, as it was in the case 1D LP. This may be related to the fact that clusters C, D and F can be obtained from B, C, and D, respectively, by adding a single peak having exactly two neighbors. On the contrary the two peaks cluster B is obtained from the single peak solution A by adding a peak having only a single neighbor. Therefore, the lines corresponding to these two spatial profiles intersect in the point M1 different from M2. Furthermore, the seven-peaks cluster can be obtained from the six-peaks one by adding a single peak having exactly three neighbors. Hence, the intersection of the lines G and F in Fig. 3b is located at the third point M3, different from M1 and M2. Similarly to the case of 1D patterns, below (above) a “Maxwell-point”, the pattern with smaller number of peaks is more (less) stable than that with greater number of peaks.

To conclude, we have shown that relative stability of clusters of close-packed peaks depends on the number of peaks in the localized pattern. More precisely, at the Maxwell point different clusters are equally stable independently of the number of peaks. Below (above) that point, clusters consisting of a larger number of peaks are less (more) stable than those with a smaller number of peaks. This means that the most stable solution is a single peak state below the Maxwell point and the infinite patterned state above this point.

M.T. is a Research Associate with the Fonds de la Recherche Scientifique F.R.S.-FNRS, Belgium. A.V. is supported by SFB 787 project of the DFG. The financial support of Fonds Emile Defay is also acknowledged.

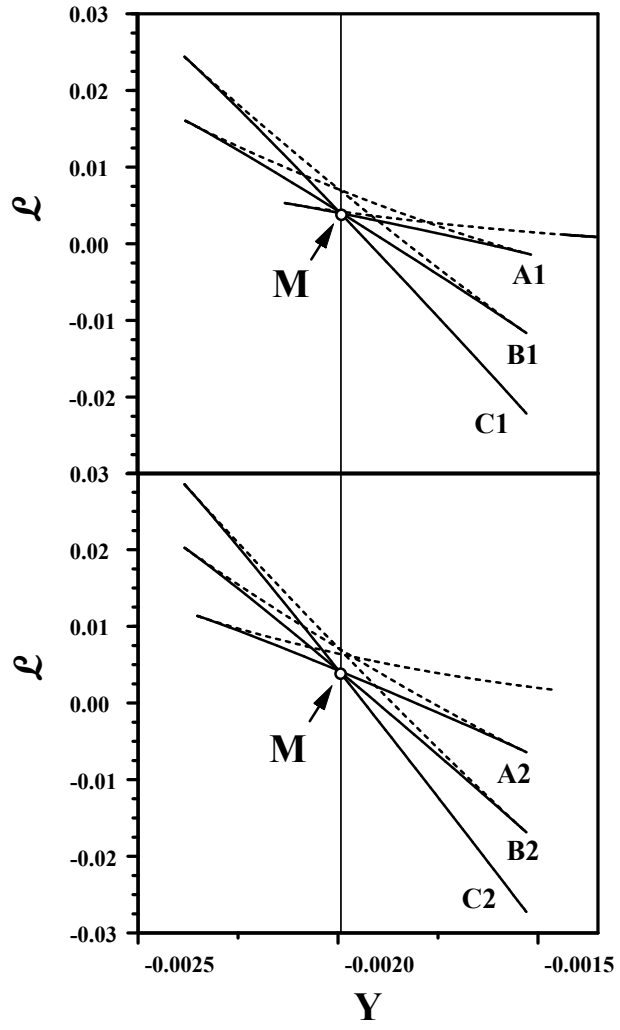

Figure 2: Lyapunov functional $\mathscr{L}$ as a function of the control parameter Y. Solid (dotted) curves correspond to stable (unstable) localized solutions. M is the Maxwell point. Parameters are the same as in Fig. 1a. The branches $A1$, $B1$, and $C1$ correspond to LP shown in Fig. 1(b). The branches $A2$, $B2$, and $C2$ correspond to LP shown in Fig. 1(c).

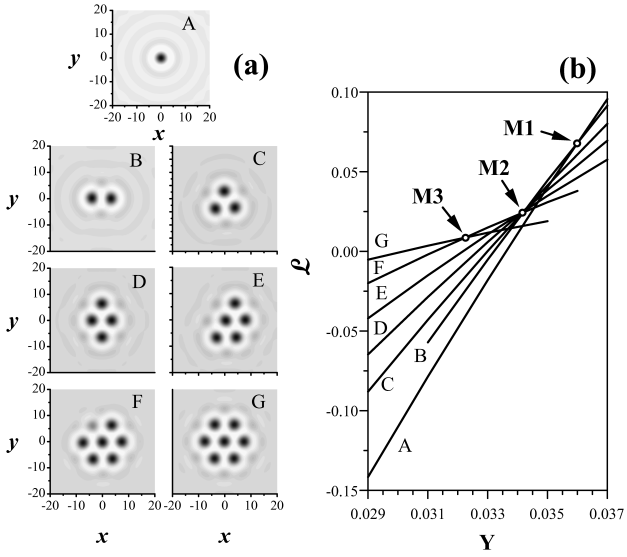

Figure 3: Stable clusters of 2D hexagonal close-packed peaks of Eq. (1) (a) and dependencies of the Lyapunov functional on the injection parameter Y for these clusters (b). M1, M2, and M3 are the intersection points. Parameters are $C = -0.05$ and $\Gamma = 3/8$. Maxima are plain black.

References

[1] V.B. Taranenko, K. Staliunas, and C.O. Weiss, Phys. Rev. A **56**, 1582 (1997); V.B. Taranenko et al., Phys. Rev. Lett. **81**, 2236 (1998).

[2] S. Barland, J.R. Tredicci, M. Brambilla, L.A. Lugiato, S. Balle, M. Guidici, T. Maggipinto, L. Spinelli, G. Tissoni, T. Knodl, M.Miller, and R. Jager, Nature **419**, 699 (2002).

[3] X. Hachair, L. Furfaro, J. Javaloyes, M. Giudici, S. Balle, J. Tredicce, G. Tissoni, L.A. Lugiato, M. Brambilla, and T. Maggipinto, Phys. Rev. A **72**, 013815 (2005).

[4] M.G. Clerc, A. Petrossian, and S. Residori, Phys. Rev. E **71**, 015205 (2005); S. Residori et al. J. Opt. B: Quantum Semiclass. Opt. **6**, S169 (2004).

[5] D. Bajoni, E. Semenova, A. Lemaître, S. Bouchoule, E. Wertz, P. Senellart, S. Barbay, R. Kuszelewicz, and J. Bloch, Phys. Rev. Lett. **101**, 266402 (2008).

[6] P. Genevet, S. Barland, M. Giudici, and J.R. Tredicce, Phys. Rev. Lett. **101**, 123905 (2009).

[7] H.R. Brand and R.J. Deissler, Phys. Rev. Lett. **63**, 2801 (1989).

[8] B. A. Malomed, Phys. Rev. A **44**, 6954 (1991); B. A. Malomed, Phys. Rev. E **58**, 7928 (1998).

[9] M. Tlidi, P. Mandel, and R. Lefever, Phys. Rev. Lett. **73**, 640 (1994).

[10] A.J. Scroggie et al., Chaos Solitons and Fractals, **4**, 1323 (1994).

[11] A.G. Vladimirov, G.V. Khodova, and N. N. Rosanov, Phys. Rev. E **63**, 056607 (2001).

[12] A.G. Vladimirov, J.M. McSloy, D.V. Skryabin, and W.J. Firth, Phys. Rev. E **65**, 046606 (2002).

[13] M. Tlidi, A.G. Vladimirov, and P. Mandel, IEEE Journal of Quantum Electronics **39**, 216 (2003).

[14] N.N. Rosanov, S.V. Fedorov, A.N. Shatsev, Phys. Rev. Lett. **95**, 053903 (2005).

[15] N.N. Rosanov, Spatial Hysteresis and Optical Patterns (Springer, Berlin, 2002).

[16] M. Tlidi, T. Kolokolnikov, and M. Taki, Focus Issue "Dissipative Localized Structures in Extended Systems", Chaos, **17** , Issue 3 (2007).

[17] N. Akhmediev and A. Ankiewicz "Dissipative Solitons: From Optics to Biology and Medicine" (Springer-Verlag, Berlin, Heidelberg, 2008).

[18] B. Schäpers, M. Feldmann, T. Ackemann, and W. Lange, Phys. Rev. Lett. **85**, 748 (2000).

[19] U. Bortolozzo, M.G. Clerc and S. Residori, New J. Phys. **11**, 093037 (2009).

[20] S. Barbay, X. Hachair, T. Elsass, I. Sagnes, and R. Kuszelewicz, Phys. Rev. Lett. **101**, 253902 (2008).

[21] A. Kaminaga, V.K. Vanag, and I.R. Epstein, J. Chem. Phys. **122**, 174706 (2005); V.K. Vanag and I.R. Epstein, Chaos **17**, 037110 (2007).

[22] L.A. Lugiato and R. Lefever, Phys. Rev. Lett. **58**, 2209 (1987).

[23] The physical meaning of the field variable U is the electric field, phytomass density or chemical concentration. The control parameter measures the input field amplitude, the aridity parameter or chemical concentration.

[24] Y. Pomeau, Physica D **23**, 3 (1986).

[25] L. Yu. Glebsky and L.M. Lerman, Internat. J. Nonlion. Sci.**5**, 424 (1995).

[26] A.R. Campneys, Physica D **112**, 158 (1998); G.W. Hunt, G.J. Lord, and Champneys, Compt. Methods Appl. Mech. Eng. **170**, 239 (1999); P. Coullet, C. Riera, and C. Tresser, Phys. Rev. Lett. **84**, 3069 (2000).

[27] Y. Nishiura and D. Ueama, Physica D **130**, 73 (1999); J. Burke and E. Knobloch, Phys. Rev. E **73**, 056211 (2006); M.G. Clerc, C. Falcon, and E. Tirapegui, Phys. Rev. Lett. 94, 148302 (2005); G. Kozyreff and S.J. Chapman, Phys. Rev. Lett. **97**, 044502 (2006); D. Gomila, A. J. Scroggie, and W.J. Firth, Physica D **227**, 70 (2007); E. Knobloch, Nonlinearity, **21**, T45 (2008); L. Gelens and E. Knobloch; Phys. Rev. E **80**, 046221 (2009).

[28] J. Burke and E. Knobloch, Chaos, **17**, 037102 (2007); W.J. Firth, L. Columbo, and T. Maggipinto, Chaos, **17**, 037115 (2007); D.J.B Lloyd, B. Sandstede, D. Avitabile, and A.R. Champneys, SIAM J. App. Dyn. 7, 1049 (2008).

[29] F. Haudin, R.G. Elias, R.G. Rojas, U. Bortolozzo, M.G. Clerc, and S. Residori, Phys. Rev. Lett. **103**, 128003 (2009).

[30] J. Swift and P.C. Hohenberg, Phys. Rev. A **15**, 319 (1977).

[31] M'F Hilali, G. Dewel, and P. Borckmans, Phys. Lett. A **217**, 263 (1996); M'F Hilali, S. Metens, P. Borckmans, and G. Dewel, Phys. Rev. E **51**, 2046 (1995).

[32] R. Lefever, N. Barbier, P. Couteron, and O. Lejeune, Journal of Theoretical Biology, **261**, 194 (2009).

[33] P. Mandel, M. Georgiou, and T. Erneux, Phys. Rev. A **47**, 4277 (1993); M. Le Berre, E. Ressayre, and A. Tallet, Quantum Semiclassic. Opt. **7**, 1 (1995).

[34] M. Tlidi, M. Georgiou, and P. Mandel, Phys. Rev. A **48**, 4605 (1993).